DNA Structures

Deutsche Ausgabe: DOI: 10.1002/ange.201504656
Internationale Ausgabe: DOI: 10.1002/anie.201504656

Single-Molecule Visualization of the Activity of a Zn^{2+}-Dependent DNAzyme**

Masayuki Endo, Yosuke Takeuchi, Yuki Suzuki, Tomoko Emura, Kumi Hidaka, Fuan Wang, Itamar Willner,* and Hiroshi Sugiyama**

Abstract: *We demonstrate the single-molecule imaging of the catalytic reaction of a Zn^{2+}-dependent DNAzyme in a DNA origami nanostructure. The single-molecule catalytic activity of the DNAzyme was examined in the designed nanostructure, a DNA frame. The DNAzyme and a substrate strand attached to two supported dsDNA molecules were assembled in the DNA frame in two different configurations. The reaction was monitored by observing the configurational changes of the incorporated DNA strands in the DNA frame. This configurational changes were clearly observed in accordance with the progress of the reaction. The separation processes of the dsDNA molecules, as induced by the cleavage by the DNAzyme, were directly visualized by high-speed atomic force microscopy (AFM). This nanostructure-based AFM imaging technique is suitable for the monitoring of various chemical and biochemical catalytic reactions at the single-molecule level.*

Catalytic nucleic acids (DNAzymes) are attracting growing scientific interest, and different applications of DNAzymes have been discussed.[1] These applications[2–7] include the use of DNAzymes as catalysts that stimulate biocatalytic transformations,[2] as amplifying labels for sensing events,[3] as catalysts that transduce logic-gate operations,[4] as biomolecular switching devices,[4a,5] and as functional units for the controlled release of substrates entrapped in nanocontainers.[6,7] One specific class of DNAzymes is metal-ion-dependent DNAzymes. Different DNA sequences dependent on metal-ion cofactors, such as Mg^{2+}, Ca^{2+}, Zn^{2+}, UO_2^{2+}, Hg^{2+}, and others, have been reported.[8,9] These metal-ion-dependent DNAzymes have been applied as amplifying labels for sensing,[10] as functional components for the construction of logic gates[11] and computing circuits, and as stimuli-responsive DNA switches.[4c,12]

High-speed atomic force microscopy (AFM) measurements were recently implemented to probe DNA nanostructures and their reactivity at the single-molecule level.[13] In these experiments, the individual unique DNA nanostructures were assembled on the DNA origami frames, and the reactions of the nanostructures were elucidated by analyzing a collection of frames. For example, DNA structural changes, including G-quadruplex reconfiguration,[14] B–Z configurational transitions,[15] and the switchable association and dissociation of photoresponsive DNA,[16] were demonstrated, and enzymatic processes on DNA nanostructures were visualized.[17] Because the target DNA strands are directly attached to the nanoscaffold, the DNA structural changes can be controlled in the nanospace by arranging the structures inside the DNA nanoscaffold.

In the present study, we used the DNA origami frame to follow the activity of a catalytic nucleic acid, a Zn^{2+}-dependent DNAzyme, at the single-molecule level. For the observation of substrate cleavage by the DNAzyme, we introduced the DNAzyme and substrate between two double-stranded DNA molecules (dsDNAs) in a DNA frame (Figure 1).[17] The DNAzyme we employed was a Zn^{2+}-ion-dependent DNAzyme that selectively cleaves the substrate DNA at a sequence-specific site (Figure 1 a).[18] We connected the DNAzyme to one supported dsDNA molecule and the substrate to another, and subsequently incorporated them into the DNA origami frame by using the four single-stranded DNA tethers as linkers (Figure 1 b). We generated two different configurations of the DNAzyme sequence/substrate pairs for insertion into the DNA frame. In the vertical configuration of the DNAzyme/substrate dsDNA in the DNA frame, the two supported dsDNA molecules were connected to the a,b and c,d sites of the DNA frame to give a structure of type **1** (Figure 1 c). In the horizontal configuration, the two dsDNA molecules were connected to the a,c and b,d sites to give a structure of type **3** (Figure 1 d).

First, we examined the cleavage of the substrate DNA by using a DNAzyme oligonucleotide (see Figures S1 and S2 in

[*] Prof. Dr. M. Endo, Prof. Dr. H. Sugiyama
Institute for Integrated Cell-Material Sciences (WPI-iCeMS)
Kyoto University
Yoshida-ushinomiyacho, Sakyo-ku, Kyoto 606-8501 (Japan)
E-mail: endo@kuchem.kyoto-u.ac.jp
hs@kuchem.kyoto-u.ac.jp
Y. Takeuchi, Dr. Y. Suzuki, T. Emura, K. Hidaka, Prof. Dr. H. Sugiyama
Department of Chemistry, Graduate School of Science
Kyoto University
Kitashirakawa-oiwakecho, Sakyo-ku, Kyoto 606-8502 (Japan)
Prof. Dr. M. Endo, Prof. Dr. H. Sugiyama
CREST (Japan) Science and Technology Agency (JST)
Sanbancho, Chiyoda-ku, Tokyo 102-0075 (Japan)
Dr. F. Wang, Prof. Dr. I. Willner
Institute of Chemistry, The Minerva Center for Biohybrid Complex Systems, The Hebrew University of Jerusalem
Jerusalem 91904 (Israel)
E-mail: willnea@vms.huji.ac.il

[**] This research was supported by a Grant-in-Aid for Scientific Research on Innovative Areas ("Molecular Robotics", grant number 24104002) from MEXT, Core Research for Evolutional Science and Technology (CREST) of JST, and JSPS KAKENHI (grant numbers 15H03837, 24225005, 26620133). I.W. is supported by the Israel Science Foundation. Financial support through research grants to M.E. from Sekisui Chemical and the Kurata Memorial Hitachi Science and Technology Foundation is also acknowledged.

Supporting information for this article is available on the WWW under http://dx.doi.org/10.1002/anie.201504656.

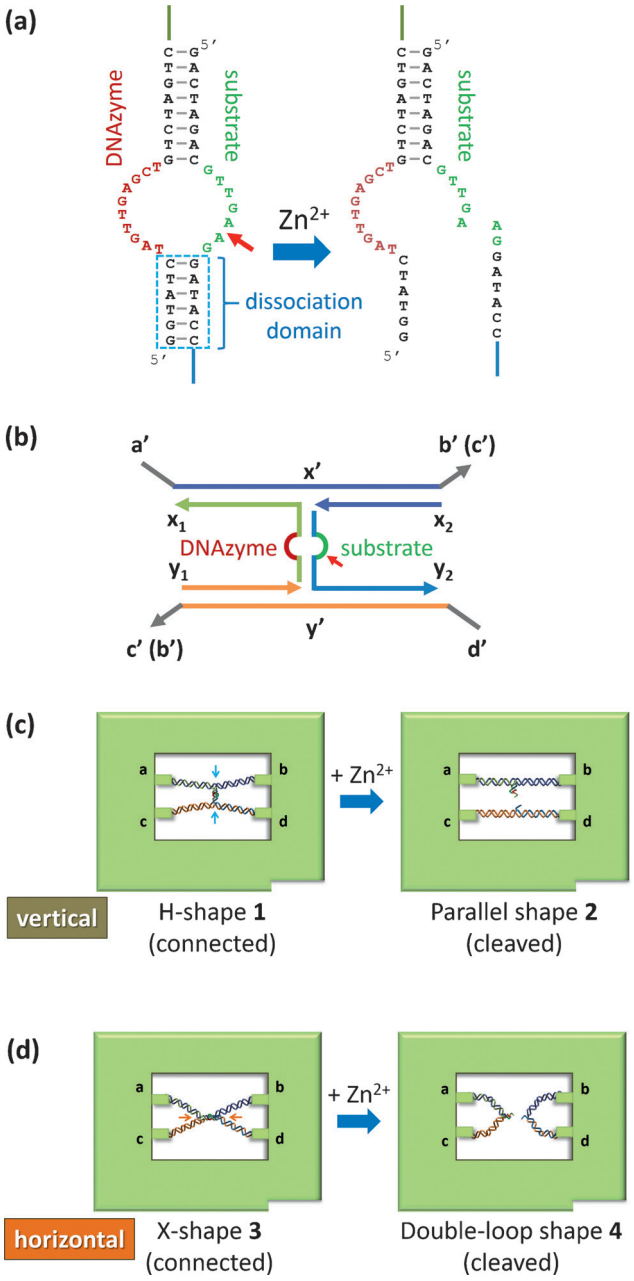

Figure 1. Single-molecule observation system for a DNAzyme-mediated cleavage reaction in a DNA frame. a) DNAzyme and substrate sequences used in the experiments. The addition of Zn^{2+} induces cleavage at a specific site (red arrow). The number of base pairs in the dissociation domain of the DNAzyme (dashed blue rectangle) was varied (4, 6, and 8 bp). b) Schematic representation of DNA strands incorporated into the DNA frame. c) Vertical configuration in the DNA frame in the initial state (left; H-shape **1**) and the product after cleavage with Zn^{2+} (right; parallel shape **2**). d) Horizontal configuration in the DNA frame in the initial state (left; X-shape **3**) and the product after cleavage with Zn^{2+} (right; double-loop shape **4**).

the Supporting Information). We conducted the reaction in a solution containing 10 mM Tris buffer (pH 7.0), 20 mM $MgCl_2$, and a metal ion at 30 °C for 30 min. The cleavage selectively occurred in the presence of Zn^{2+}, whereas no cleavage was observed in the presence of other ions, such as Cu^{2+} or Ni^{2+}, as reported previously (see Figure S1 a).[18] We then examined the reaction in the DNA nanostructure under the same reaction conditions. The DNAzyme and substrate DNA supported by two dsDNA molecules were introduced into a DNA frame by pre-annealing the DNA components in a solution containing 10 mM Tris buffer (pH 7.0) and 20 mM $MgCl_2$ (see Figure S3). After their assembly, the structures were observed by AFM. The two dsDNAs were connected to the DNA frame in >90% yield (Figure 2). A central H-shaped DNAzyme/substrate dsDNA construct in the vertical configuration was clearly identified in the intact structure (Figure 2 a; see also Figure S4). The DNAzyme and substrate DNA supported by two dsDNAs were also assembled in the DNA frame in the horizontal configuration (see Figure S9). Again, the center dsDNA was clearly identified, and the whole structure was observed as an X-shape (Figure 2 e; see also Figure S10). The DNAzyme/substrate dsDNA in the vertical and horizontal configurations could be clearly visualized between the two supported dsDNAs in the DNA frame (Figure 2 a,e).

Next, we examined the cleavage reaction of the substrate DNA in the respective DNA frames. The reaction was performed in the presence of 2 mM $ZnCl_2$ at 30 °C for 30 min. Upon incubation with Zn^{2+} in the DNA frames, the separation of the central part of the DNAzyme/substrate dsDNA units were clearly observed (Figure 2). In the case of the vertical configuration, we observed the separation of the two supported dsDNAs to give a parallel shape (Figure 2 b; see also Figure S5). We compared the effect of the number of base pairs in the dissociation domain on the separation, with 4, 6, and 8 base pairs (bp; Figure 2 c; see also Figures S6–S8). After incubation with Zn^{2+}, the proportion of structures with the parallel shape increased as the number of base pairs decreased from 8 to 4 bp, and the observed separation with the 8 bp dissociation domain was modest. These results show that the number of base pairs in the dissociation domain affects the separation in the DNA frame after cleavage. We examined the time-dependent formation of the parallel shape in the DNA frame by using DNAzymes with a 4 and 6 bp dissociation domain (Figure 2 d; see also Figures S7 and S8). In both cases, the reactions were saturated by a reaction time of around 30 min, and the formation of the parallel shape occurred in higher yield with a DNAzyme with a 4 bp dissociation domain than with a 6 bp domain. The observed rate constants for the formation of the parallel shape by DNAzymes with 4 and 6 bp were 0.18 and 0.068 min^{-1}, respectively, thus indicating that the dissociation of the cleaved substrate and DNAzyme directly affects the kinetics of the formation of the parallel shape. In the cases of the horizontal configuration, we also observed the separation of the two supported dsDNAs, which upon cleavage formed a double-loop shape (Figure 2 f; see also Figure S11). We also observed an effect of the dissociation domain on the formation of the double loop. The trend for the separation was similar to that observed for the vertical configuration (Figure 2 g; see also Figures S12–S14). The observed rate constants for double-loop formation with 4 and 6 bp dissociation domains were 0.17 and 0.094 min^{-1}, respectively; again this result was similar to that for the vertical configuration

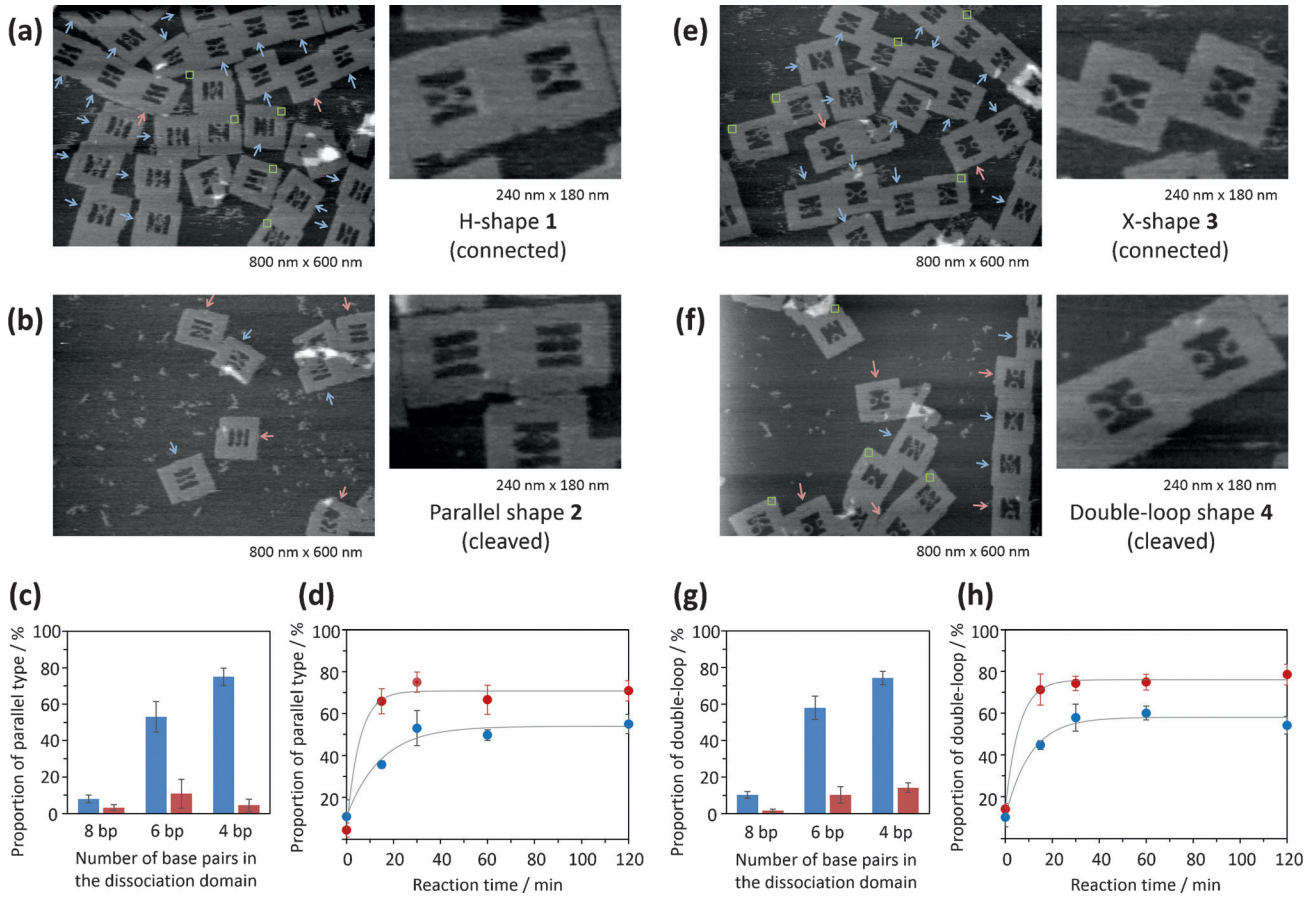

Figure 2. AFM images corresponding to the Zn^{2+}-dependent DNAzyme-catalyzed cleavage of the substrate DNA in the DNA frames. a) AFM images of DNA frames in the vertical configuration in the initial state. Blue and red arrows indicate DNA frames containing H-shaped and parallel-shaped dsDNAs **1** and **2**, respectively. Green rectangles indicate DNA frames containing unclear constructs. b) AFM images of DNA frames in the vertical configuration after incubation with $ZnCl_2$. c) Extent of substrate cleavage by DNAzymes with 4, 8, or 6 bp dissociation domains in the vertical configuration. Red and blue bars indicate the proportion of constructs with the parallel shape initially and after incubation with Zn^{2+} at 30 °C for 30 min, respectively. d) Time-dependent formation of parallel shape structures by DNAzymes with a dissociation domain comprising 4 (red circles) and 6 bp (blue circles). Error bars represent mean ± standard deviation for three independent experiments. e) AFM images of DNA frames with the horizontal configuration in the initial state. Blue and red arrows indicate DNA frames containing X-shaped and double-loop-shaped dsDNAs **3** and **4**, respectively. f) AFM images of DNA frames with the horizontal configuration after incubation with Zn^{2+}. g) Substrate cleavage by DNAzymes with 4, 8, or 6 bp dissociation domains in the vertical configuration. Red and blue bars indicate the proportion of constructs with the double-loop shape initially and after incubation, respectively. h) Time-dependent formation of double-loop shape structures by DNAzymes with a dissociation domain comprising 4 (red circles) and 6 bp (blue circles).

(Figure 2h). The formation of the parallel and double-loop structures in the DNA frame was derived from the dissociation of the cleaved substrate from the DNAzyme strand. Considering the rate constant of substrate cleavage with the same DNAzyme in an ensemble state (0.48 min^{-1}; see Figure S1b), the additional dissociation step affects the observed rate constants for the formation of the parallel and double-loop structures during the reaction in the DNA frames.

When the DNAzyme/substrate dsDNA structures are incorporated in the DNA frame, the lengths of the center DNAzyme/substrate dsDNA supported by the two dsDNAs are different in the two configurations, and this difference should affect the reactions. We measured the lengths of the center dsDNA in the vertical and horizontal configurations in the AFM images. The center-to-center distances between the two supported dsDNAs in these configurations were (13.5 ± 1.8) and (10.7 ± 2.0) nm, respectively (Figure 2a,e; see also Figure S15). Although the tension imposed on the center dsDNA in the vertical configuration should be higher than that in the horizontal configuration, the observed rate constants were similar. The results suggest that the catalytic activity was preserved in both configurations, even though the DNAzyme/substrate was extended differently by the two supported strands.

Finally, we examined the imaging of the single-molecule cleavage reaction by the DNAzyme by high-speed AFM. We prepared a sample in the absence of Zn^{2+} and observed the sample in the presence of Zn^{2+}. The prepared sample was adsorbed on mica, and then the sample was examined in an observation buffer containing Zn^{2+}. First, we examined the vertical configuration. We found that the H-shaped structure in the vertical configuration changed into the separated dsDNAs during AFM scanning (arrow in Figure 3a; see also Figure S16a). The dsDNA separated, and the corresponding

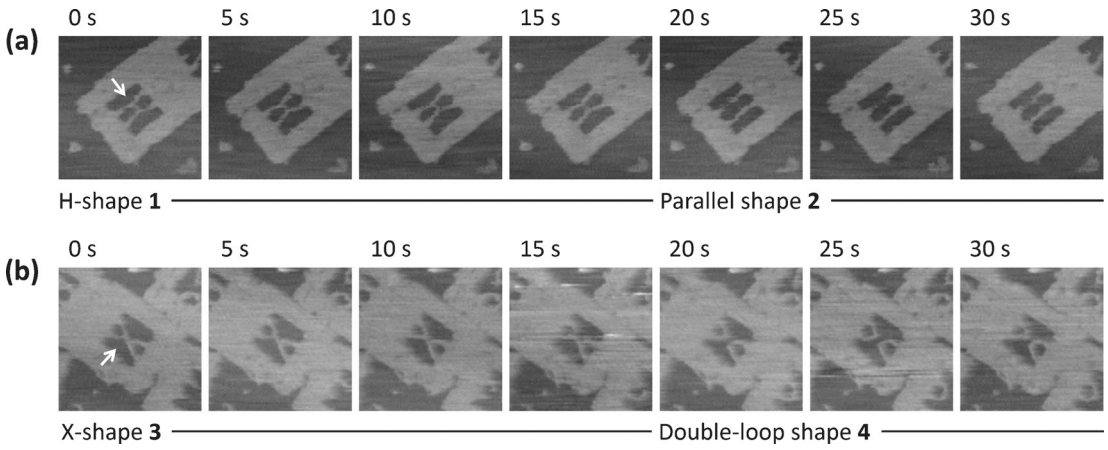

Figure 3. Time-lapse AFM images for the dissociation of DNA strands as induced by the cleavage of substrate DNA by the DNAzyme in the DNA frames. a) Time-lapse images of the reaction in the vertical configuration in the presence of $ZnCl_2$. b) Time-lapse images of the reaction in the horizontal configuration in the presence of $ZnCl_2$. The time point 0 s was chosen arbitrarily during AFM scanning. Scanning rate: 0.2 frames s^{-1}; image size: 150×150 nm.

conversion of the H-shaped structure into two separated parallel dsDNAs was clearly observed at a reaction time of 20 s (Figure 3a). In the case of the horizontal configuration, we also observed the structural conversion from an X-shaped structure into two separated loops at a reaction time of 20 s (arrow in Figure 3b; see also Figure S16b). By tracking the successive images of the shapes of the target dsDNAs in the DNA frame, we found that the separation of the center dsDNAs occurred within 5 s. By using this observation system, we could clearly monitor the DNAzyme reactions and the subsequent separation of the supported dsDNAs and formation of the parallel and double-loop structures at single-molecule resolution.

In conclusion, we have demonstrated the single-molecule imaging of the cleavage and dissociation of dsDNA by a Zn^{2+}-dependent DNAzyme within a DNA nanostructure. The DNA frame could compartmentalize the target molecules for the detailed observation of the individual reactions. The reactions were monitored by observing the configuration change of the dsDNAs incorporated in the DNA frames. The dynamic movements of the DNA strands, as induced by cleavage by the DNAzyme, were visualized in the DNA frames by high-speed AFM. The versatile observation system described herein could be a novel approach for monitoring target chemical and biochemical reactions that are designed to induce structural arrangements of multiple DNA strands in designed DNA nanospaces.

Keywords: DNA origami · DNA structures · DNAzymes · high-speed atomic force microscopy · single-molecule imaging

How to cite: *Angew. Chem. Int. Ed.* **2015**, *54*, 10550–10554
Angew. Chem. **2015**, *127*, 10696–10700

[1] a) R. R. Breaker, G. F. Joyce, *Chem. Biol.* **1994**, *1*, 223–229; b) I. Willner, B. Shlyahovsky, M. Zayats, B. Willner, *Chem. Soc. Rev.* **2008**, *37*, 1153–1165; c) M. Famulok, J. S. Hartig, G. Mayer, *Chem. Rev.* **2007**, *107*, 3715–3743; d) G. F. Joyce, *Angew. Chem. Int. Ed.* **2007**, *46*, 6420–6436; *Angew. Chem.* **2007**, *119*, 6540–6557; e) J. Andreasson, S. D. Straight, S. Bandyopadhyay, R. H. Mitchell, T. A. Moore, A. L. Moore, D. Gust, *J. Phys. Chem. C* **2007**, *111*, 14274–14278.

[2] a) E. Golub, R. Freeman, I. Willner, *Angew. Chem. Int. Ed.* **2011**, *50*, 11710–11714; *Angew. Chem.* **2011**, *123*, 11914–11918; b) Z.-G. Wang, P. Zhan, B. Ding, *ACS Nano* **2013**, *7*, 1591–1598; c) M. Wilking, U. Hennecke, *Org. Biomol. Chem.* **2013**, *11*, 6940–6945.

[3] a) R. Freeman, J. Girsh, I. Willner, *ACS Appl. Mater. Interfaces* **2013**, *5*, 2815–2834; b) Y. Du, B. Li, E. Wang, *Acc. Chem. Res.* **2013**, *46*, 203–213; c) Y. V. Gerasimova, D. M. Kolpashchikov, *Chem. Biol.* **2010**, *17*, 104–106; d) G. Pelossof, R. Tel-Vered, I. Willner, *Anal. Chem.* **2012**, *84*, 3703–3709; e) R. Orbach, F. Wang, O. Lioubashevsky, R. D. Levine, F. Remacle, I. Willner, *Chem. Sci.* **2014**, *5*, 3381–3387; f) F. Wang, C.-H. Lu, I. Willner, *Chem. Rev.* **2014**, *114*, 2881–2941.

[4] a) S. Shimron, N. Magen, J. Elbaz, I. Willner, *Chem. Commun.* **2011**, *47*, 8787–8789; b) C. Teller, S. Shimron, I. Willner, *Anal. Chem.* **2009**, *81*, 9114–9119; c) J. Elbaz, S. Shimron, I. Willner, *Chem. Commun.* **2010**, *46*, 1209–1211; d) G. Seelig, D. Soloveichik, D. Y. Zhang, E. Winfree, *Science* **2006**, *314*, 1585–1588; e) A. Padirac, T. Fujii, Y. Rondelez, *Curr. Opin. Biotechnol.* **2013**, *24*, 575–580; f) L. Qian, E. Winfree, *Science* **2011**, *332*, 1196–1201; g) L. Qian, E. Winfree, J. Bruck, *Nature* **2011**, *475*, 368–372; h) R. R. Breaker, *Nat. Biotechnol.* **1997**, *15*, 427–431.

[5] a) B. Ge, Y. C. Huang, D. Sen, H. Z. Yu, *Angew. Chem. Int. Ed.* **2010**, *49*, 9965–9967; *Angew. Chem.* **2010**, *122*, 10161–10163; b) X. Liu, A. Niazov-Elkan, F. Wang, I. Willner, *Nano Lett.* **2013**, *13*, 219–225.

[6] M. Moshe, J. Elbaz, I. Willner, *Nano Lett.* **2009**, *9*, 1196–1200.

[7] a) C. H. Lu, X. J. Qi, R. Orbach, H.-H. Yang, I. Mironi-Harpaz, D. Seliktar, I. Willner, *Nano Lett.* **2013**, *13*, 1298–1302; b) Z. Zhong, D. Balogh, F. Wang, I. Willner, *J. Am. Chem. Soc.* **2013**, *135*, 1934–1940.

[8] a) R. R. Breaker, G. F. Joyce, *Trends Biotechnol.* **1994**, *12*, 268–275; b) J. Tang, R. R. Breaker, *Proc. Natl. Acad. Sci. USA* **2000**, *97*, 5784–5789.

[9] a) J. W. Liu, A. K. Brown, X. L. Meng, D. M. Cropek, J. D. Istok, D. B. Watson, Y. Lu, *Proc. Natl. Acad. Sci. USA* **2007**, *104*, 2056–2061; b) J. Liu, Y. Lu, *J. Am. Chem. Soc.* **2007**, *129*, 9838–9839.

[10] a) C. H. Fan, K. W. Plaxco, A. J. Heeger, *Proc. Natl. Acad. Sci. USA* **2003**, *100*, 9134–9137; b) F. Wang, J. Elbaz, R. Orbach, N. Magen, I. Willner, *J. Am. Chem. Soc.* **2011**, *133*, 17149–17151.

[11] a) M. N. Stojanovic, T. E. Mitchel, D. Stefanovic, *J. Am. Chem. Soc.* **2002**, *124*, 3555–3561; b) M. N. Stojanovic, D. Stefanovic,

Nat. Biotechnol. **2003**, *21*, 1069 – 1074; c) L. Wang, J. Zhu, L. Han, L. Jin, C. Zhu, E. Wang, S. Dong, *ACS Nano* **2012**, *6*, 6659 – 6666; d) R. Orbach, L. Mostinski, F. Wang, I. Willner, *Chem. Eur. J.* **2012**, *18*, 14689 – 14694; e) R. Orbach, F. Remacle, R. D. Levine, I. Willner, *Proc. Natl. Acad. Sci. USA* **2012**, *109*, 21228 – 21233; f) J. M. Picuri, B. M. Frezza, M. R. Ghadiri, *J. Am. Chem. Soc.* **2009**, *131*, 9368 – 9377; g) N. C. Gianneschi, M. R. Ghadiri, *Angew. Chem. Int. Ed.* **2007**, *46*, 3955 – 3958; *Angew. Chem.* **2007**, *119*, 4029 – 4032; h) Y. Benenson, T. Paz-Elizur, R. Adar, E. Keinan, Z. Livneh, E. Shapiro, *Nature* **2001**, *414*, 430 – 434; i) Y. Benenson, B. Gil, U. Ben-Dor, R. Adar, E. Shapiro, *Nature* **2004**, *429*, 423 – 429; j) R. Adar, Y. Benenson, G. Linshiz, A. Rosner, N. Tishby, E. Shapiro, *Proc. Natl. Acad. Sci. USA* **2004**, *101*, 9960 – 9965; k) H. Lederman, J. Macdonald, D. Stefanovic, M. N. Stojanovic, *Biochemistry* **2006**, *45*, 1194 – 1199.

[12] M. Zhou, X. Liang, T. Mochizuki, H. Asanuma, *Angew. Chem. Int. Ed.* **2010**, *49*, 2167 – 2170; *Angew. Chem.* **2010**, *122*, 2213 – 2216.

[13] a) M. Endo, H. Sugiyama, *Acc. Chem. Res.* **2014**, *47*, 1645 – 1653; b) A. Rajendran, M. Endo, H. Sugiyama, *Chem. Rev.* **2014**, *114*, 1493 – 1520; c) A. Rajendran, M. Endo, H. Sugiyama, *Angew. Chem. Int. Ed.* **2012**, *51*, 874 – 890; *Angew. Chem.* **2012**, *124*, 898 – 915.

[14] a) Y. Sannohe, M. Endo, Y. Katsuda, K. Hidaka, H. Sugiyama, *J. Am. Chem. Soc.* **2010**, *132*, 16311 – 16313; b) A. Rajendran, M. Endo, K. Hidaka, H. Sugiyama, *Angew. Chem. Int. Ed.* **2014**, *53*, 4107 – 4112; *Angew. Chem.* **2014**, *126*, 4275 – 4279.

[15] a) A. Rajendran, M. Endo, K. Hidaka, H. Sugiyama, *J. Am. Chem. Soc.* **2013**, *135*, 1117 – 1123; b) M. Endo, M. Inoue, Y. Suzuki, C. Masui, H. Morinaga, K. Hidaka, H. Sugiyama, *Chem. Eur. J.* **2013**, *19*, 16887 – 16890.

[16] M. Endo, Y. Yang, Y. Suzuki, K. Hidaka, H. Sugiyama, *Angew. Chem. Int. Ed.* **2012**, *51*, 10518 – 10522; *Angew. Chem.* **2012**, *124*, 10670 – 10674.

[17] a) M. Endo, Y. Katsuda, K. Hidaka, H. Sugiyama, *J. Am. Chem. Soc.* **2010**, *132*, 1592 – 1597; b) M. Endo, Y. Katsuda, K. Hidaka, H. Sugiyama, *Angew. Chem. Int. Ed.* **2010**, *49*, 9412 – 9416; *Angew. Chem.* **2010**, *122*, 9602 – 9606; c) Y. Suzuki, M. Endo, Y. Katsuda, K. Ou, K. Hidaka, H. Sugiyama, *J. Am. Chem. Soc.* **2014**, *136*, 211 – 218.

[18] H. Gu, K. Furukawa, Z. Weinberg, D. F. Berenson, R. R. Breaker, *J. Am. Chem. Soc.* **2013**, *135*, 9121 – 9129.

Received: May 22, 2015
Published online: July 17, 2015